Morphological, molecular and functional differences of adult bone marrow- and adipose-derived stem cells isolated from rats of different ages

Cristina Mantovani[a,b,c], Stefania Raimondo[d], Maryam S. Haneef[a], Stefano Geuna[d], Giorgio Terenghi[a], Susan G. Shawcross[a,N], Mikael Wiberg[b,c]

[a]*Blond McIndoe Laboratories, School of Biomedicine, The University of Manchester, Room 3,106 Stopford Building, Oxford Road, Manchester M13 9PT, Academic Health Science Centre, Faculty of Medicine and Human Sciences, United Kingdom*
[b]*Department of Integrative Medical Biology and Surgical & Perioperative Science, Umea˚ University, Umea˚, Sweden* [c]*Department of Surgical & Perioperative Science, Umea˚ University, Umea˚, Sweden*
[d]*Dipartimento di Scienze Cliniche e Biologiche, University of Turin, Italy*

Abstract

Adult mesenchymal stem cells have self-renewal and multiple differentiation potentials, and play important roles in regenerative medicine. However, their use may be limited by senescence or age of the donor, leading to changes in stem cell functionality. We investigated morphological, molecular and functional differences between bone marrow-derived (MSC) and adipose-derived (ASC) stem cells isolated from neonatal, young and old rats compared to Schwann cells from the same animals. Immunocytochemistry, RT-PCR, proliferation assays, western blotting and transmission electron microscopy were used to investigate expression of senescence markers. Undifferentiated and differentiated ASC and MSC from animals of different ages expressed Notch-2 at similar levels; protein-38 and protein-53 were present in all groups of cells with a trend towards increased levels in cells from older animals compared to those from neonatal and young rats. Following co-culture with adult neuronal cells, dMSC and dASC from animals of all ages elicited robust neurite outgrowth. Mitotracker^{S} staining was consistent with ultrastructural changes seen in the mitochondria of cells from old rats, indicative of senescence. In conclusion, this study showed that although the cells from aged animals expressed markers of senescence, aged MSC and ASC differentiated into SC-like cells still retain potential to support axon regeneration.

Introduction

During peripheral nerve injury and regeneration, Schwann cells (SC) play an important role by promoting axon elongation through secretion of tropic and trophic factors, and by enveloping newly regrowing axon with myelin [1]. In previous studies, we have shown that adult mesenchymal stem cells originating from either bone marrow (MSC) [2] or from adipose tissue (ASC) [3] can be differ-entiated to SC-like cells. Both differentiated MSC (dMSC) and ASC (dASC) show morphological, biochemical and functional character-istics of SCs, and importantly they secrete growth factors [4,5] and synthesise myelin proteins [6]. Experimentally, both dMSC and dASC have been shown to promote nerve regeneration to levels compar-able to those of SC [7].

In vitro, differentiated adult mesenchymal stem cells show pro-liferation capacity, but it has been suggested that the therapeutic potential of stem cells, due to bioactive growth factor secretion and stimulation of neo-angiogenesis, may be limited by their senes-cence, or biological aging, and by the age of the donor [8]. Recent reports indicate that aging is linked to a decline in the number of stem cells found in bone marrow aspirate [9] and of their potential to proliferate and differentiate [10–12]. The loss of functionality of stem cells isolated from animals of different ages is accompanied by a range of age-related biochemical changes in their niche tissue [13]. Cells from aged animals have been shown to accumulate oxidative damage and impaired mitochondrial function [14]. This variation in the functionality of the resident stem cells could be associated with a decline of the regenerative response due to the environmental cues, and to a lack of response to extrinsic signals that normally lead the stem cells to participate in tissue repair.

It is still unclear if stem cell activation is influenced by extra-cellular signals from the niche and if this stimulation is influenced by the aging process of the body. Early studies of cellular senescence showed that somatic cells can divide for a limited number of times [15]. When this limit is reached, the cells reduce replication and remain viable, but they are not capable of re-entering the cells cycle independently of stimuli

received from their surrounding environ-ment [16]. The *senescence* state is defined as a state during which the cells can no longer divide and it is quite distinct from the *quiescent* state, where cells are temporarily non-proliferative, but can be induced to divide by appropriate stimuli. These two distinct processes seem to be very important in ageing. Different markers have been proposed to identify the terminal cycles of cells in tissue samples from different ages which can be used to evaluate the relationship between aging and senescent cells. During the past few years researchers have investigated the pathways involved telomere shortening and upregulation of p38, p53 and other senescence markers [17].

The mitogen-activated protein kinase (MAPK) p38 is strongly activated by stress. It also appears to play important roles in immune response and in the regulation of cell survival and differentiation [18]. In addition to promoting cell death, p38 MAPK signalling has been shown to enhance cell growth and survival, but the mechanism of p38 MAPK activation with advanced age remains unclear. A role for p38 MAPK, using experimentally modulated aging, has been suggested in several cell types, including hematopoietic stem cells [19].

Protein p53 is normally expressed at a low level in the cell due to the action of ubiquitin ligase MDM2, which promotes its degradation. Whilst p53 is activated by various stimuli, such as stress [20], its induction does not always lead to cellular senescence. This casts doubt upon the role of p53 in the senescence programme and indicates that it may suppress senescence by converting the response to quiescence [21]. Upregulation of p53 leads to cell cycle arrest and, as a conse-quence, to the initial step of cellular senescence [22]. In the aging process of an organism, p53 signalling seems to decline as the efficiency of p53-mediated responses to cellular stresses decreases during aging [23].

The Notch gene encodes members of a family of four receptors regulating cell–cell interactions. Notch signalling seems to influ-ence important roles in many types of stem cells [8]. Adult stem cells have limited self-renewal and proliferative potential, which decreases with the advancing age of the organism [24]. This activation is regulated by Notch signalling pathways, as shown by the correlation between the decreasing of Notch signalling and the lack of regeneration in damaged muscles. Moreover, this decline in regeneration can be reversed by improving Notch expression and activation [25].

Mitochondria are the central energy generation components of cells. During their normal activity, mitochondria generate unstable reactive oxygen species (ROS) which may damage both the mitochondrion itself and other components of the cell, and this damage plays an important role in aging [26]. Mitochondria are crucial to the physiology of the cell primarily because they supply energy in the form of ATP, but they may also become involved in the process of cell death [27]. The mitochondrial population within a cell appears either as a continuous thread-like shape (mitochondrial fusion) or as short fragmented forms (mitochondrial fission) [28]. Mitochondrial fission has been implicated in the process of cell death, as mitochondrial frag-mentation precedes cytochrome C release, which initiates the apoptotic cascade reaction [29]. Thus, inhibition of mitochondrial fission may promote cell survival [30]. The mechanism involved in the regulation of mitochondrial fission and fusion is still not completely clear, but these antagonistic events may be involved in the process of aging and senescence [26]. Indeed, mitochon-dria play an essential role in life and death in all cells of most tissues and their function is fundamental in the process of cell differentiation [31]. In addition to the their traditionally described anabolic/catabolic roles, such as the production of ATP or synthesising lipids, mitochondria also appear to regulate a variety of cellular processes such as cell proliferation and aging in many cell types [32]. Self-renewal of stem cells frequently entails a resistance to the cellular senescence, as mature differ-entiated cells lose their ability to proliferate after a specific number of cell divisions [33]. In adult primate adipose-derived stem cells, low passage cell cultures contain a high proportion of undifferentiated stem cells which have significant perinuclear clustering of mitochondria, when compared to late passage number cells [34].

Taken together these data suggest that aging of the donor may result in changes of stem cell properties and functionality. In this study it was of interest to determine the morphological, mole-cular and functional differences of MSC and ASC isolated from animals of different ages, which might indicate physiological senescence of these cells. Using various markers and morpholo-gical tests, we investigated both undifferentiated and differen-tiated SC-like MSC and ASC from neonatal, adult and old rats, and compared them with SCs from the same animals.

Materials and methods

Cell harvesting and differentiation

SC, MSC and ASC were harvested from Wistar rats of different ages – new born (neonatal puppies), adult young rat (10 months) and old rats (20 months) – using protocols described elsewhere [2,3]. The animals were killed by cervical dislocation and all procedures were carried out according to the Home Office Act 1986.

MSC and ASC were stimulated towards glial differentiation using a well established protocol [2,3]. Briefly, sub-confluent undifferentiated MSC (uMSC) and ASC (uASC) were cultured in stem cell growth medium (SCGM) containing 1 MM B-mercap-toethanol for 24 h. The cells were washed and the medium replaced with fresh medium supplemented with all-*trans*-reti-noic acid (35 ng/ml) for 3 days. The medium was replaced with the addition of platelet-derived growth factor PDGF, 200 ng/ml; Sera Laboratories International, UK), basic fibroblast growth factor (bFGF, 10) Sera Laboratories International, UK) 5μM Forskolin (Sigma UK) and glial growth factor (GGF2 126 ng/ml, Acorda Therapeutics, USA), and incubated for 14 days with replacement of medium containing the above growth factors every 72 h

Alamar Blue™ assay

The metabolic activity of cells from animals of different ages and at different number of passages was measured using the Alamar BlueTM assay (Serotec, UK), which is indicative of the cell proliferation rate. SC, uMSC, dMSC, uASC and dASC were grown in 75 cm2 flasks until they reached confluence. At this point the cells were trypsinised, counted and seeded into a new flask at the density of 5 _ 105 cells in a 75 cm2 flask. The cell proliferation rates were assayed at passage 1 (P1), 5 (P5), 10 (P10), 15 (P15) and 20 (P20). For this assay, cells from each passage stage were seeded into 12-well plates at a density of 2 _ 103 cells per well. Alamar BlueTM (10% v/v) was added to the wells on day 7 of culture before the cells became confluent. Wells containing medium only (no cells) acted as a baseline control. Following the addition of Alamar blueTM, the cells were incubated for 14 h and the colour change quantified by measuring the difference in spectral absorbance (D-absorbance) at 570 nm (reduced form) and 595 nm (oxidised form) wavelengths of light for each time point. A MRX-II plate reader/spectrometer was used to measure D-absorbance, the value of the difference between the two readings being directly proportional to the cellular metabolic activity. Data were expressed as percentage of the values detected in the baseline controls.

Neuronal transwell co-culture

Dissociated dorsal root ganglia (DRG) neurons from adult young rats were cultured in 24-well plates on laminin-coated glass coverslips (Scientific Laboratories Supplies, UK). SC, dMSC or dASC from animal of different ages (neonatal, young and old) were seeded onto 0.1 Mm pore-size membrane transwell inserts (BD Falcon, UK). All cells types were seeded at a density of 42,000 cells/inserts with stem cell growth medium plus the required growth factors. The cells seeded on the insert were cultured at 37 1C in 5% CO_2 for 24 h. The co-cultures were then set up by gently placing the transwell inserts in the wells containing the neurons supplemented with normal BS medium. Negative con-trols comprised neurons cultured in normal BS medium with an overlying insert containing only the medium used to culture the cells under investigation. The co-culture was maintained for 24 h after which the neurons were fixed in 4% (w/v) PFA/PBS and immunostained with anti-BIII-tubulin antibody (see below) for analysis of neurite outgrowth.

Reverse transcription-polymerase chain reaction (RT-PCR)

Total RNA was isolated from cultures of SC, uMSC, dMSC, uASC and dASC obtained from neonatal, young and old rats. The cells were cultured in a 75 cm^2 flasks until confluent (passage 7). After trypsinisation the cells were washed in sterile PBS, centrifuged at 200*g* for 5 min and the pellet washed again in PBS. RNA extraction from cell pellets of 4 _ 10^6cells was performed using the RNeasy (Qiagen, UK) mini kit. Oligonucleotide primer pairs (Sigma Genosys, UK) and a Qiagen one-step RT-PCR kit (Qiagen) were used to reverse transcribe and amplify a region of the Notch-2 transcript (forward 5^0–TTTGCTGTCGGAAGACGACC-3^0; reverse 5^0–GCCCATGTTGTCCTGGGCGT-3^0; GenBank ID: NM_ 024358.1) and the housekeeping gene B-actin transcript (forward 5^0–CACCACAGCTGAGAGGGAAATCGTGCGTGA-3^0; reverse 5^0- ATT-TGCGGTGCACGATGGAGGGGCCGGACT – 3^0; Genbank ID: NM_ 031144.2). The B-actin transcript levels were used to assess the quality of the RNA templates for RT-PCR and to normalise transcript levels between

RNA preparations. A master mix was prepared in RNase-free water to give the final concentration of components: 1 _ Qiagen OneStep RT-PCR Buffer, 400 MM of each dNTPs, 0.6 MM of forward primer, 0.6 MM of reverse primers, 5–10 units of Qiagen One-step Enzyme mix and 1 ng template RNA or RNase-free water (negative control). An MJ Research PTC-200 (gradient) thermal cycler (MJ Research Inc, USA) was used for all reactions. The cycling parameters were as follow: a reverse transcription step of 50 1C for 30 min followed by a denaturation/reverse transcriptase inactivation step of 95 1C for 15 min then 35 cycles of denaturation (95 1C, 30 s), primer annealing (65 1C, 30 s—for both primer pairs) and primer exten sion (72 1C, 1 min) followed by final extension incubation (72 1C, 5 min). Qualitative assessment of the quantity and length of the amplicons was determined by 2% (w/v) agarose (Melford Labora tories, UK) gel electrophoresis. The agarose gels were soaked in 0. 1% (v/v) GelRed™ solution (Cambridge Bioscience Ltd., UK) solution for 10 min and images captured using an AlphaImager 2200 (AlphaInnotech Inc., USA) gel documentation system with UV transillumination.

Western blot assay

Whole cell lysates for protein assay were prepared from con-fluent cultures (passage 7) of the different types (SC, uMSC, dMSC, uASC and dASC) of cells from neonatal, young and old rats. The cells were retrieved from the culture media by an initial centrifugation step at 200*g* for 5 min, the pellets were washed in sterile PBS and re-centrifuged. The cell pellets were re-suspended into 100 Ml lysis buffer (100 mM PIPES, 5 mM $MgCl_2$, 20% (v/v) glycerol, 0.5% (v/v) Triton-X, 5 mM EGTA, with 0.005% (v/v) protease inhibitors (Sigma)) and the slurry transferred into sterile Eppendorf-type microtubes (Starlab, UK) and left for 15 min on ice, then centrifuged at 600*g* for 5 min. Gels were cast and run using Bio-Rad mini-gel apparatus (Mini-Protean^S 3 Cell vertical electrophoresis system, Bio-Rad, USA) and 15% (v/v) acrylamide (37.5:1) gels were used to resolve the proteins p38 and p53. Equal amounts of protein (10 Mg per well) isolated from SC, uMSC, dMSC, uASC and dASC were loaded onto the stacking gel and electrophoresed at 120 V for 1 h 30 min. The separated proteins were transferred to Hybond ECL nitrocellulose mem-branes (GE Healthcare, UK), and transfer confirmed by staining with Ponceau red (Sigma). The membranes were gently agitated for 2 h in blocking buffer containing 5%(w/v) non-fat milk powder (Marvel™) in TBS (10 mM Tris pH7.5, 100 mM NaCl, 0.1%(v/v) Tween-20, Sigma) and incubated with primary anti-body (anti-p38A recognising the phosphorylated protein, mouse monoclonal, 1:2000, BD Biosciences, UK; anti-p53 mouse mono-clonal antibody, 1:250, Abcam, UK) overnight at 4 1C. The following day the membranes were washed and incubated for 1 h with HRP-conjugated secondary antibodies. Finally, the membranes were treated with the ECL chemiluminescent sub-strate (GE Healthcare) for 1 min and exposed to Kodak XOMAT light sensitive film.

Immunocytochemistry

Passage 4 uMSC and uASC from neonatal, young and old rats, cultured on 32 mm diameter coverslips (SLS, UK) were fixed in 4% (w/v) PFA/PBS solution for 30 min at RT. The cells were permeabalised in 0.2% (v/v). Triton-X in PBS and background staining was blocked for 1 h in a solution of normal horse serum (diluted 1:100, Sigma). The cells were incubated overnight with primary antibodies against Stro1 (diluted 1:50, mouse mono-clonal, R&D, UK) at 4 1C. The following day, the cells were washed 3 times for 5 min in PBS and incubated at room temperature for 2 h with secondary antibodies (FITC-conjugated horse anti-mouse, diluted 1:100, Vector Laboratories, UK). Following further PBS washes, the preparations were mounted using Vectashield™ for fluorescence with DAPI (Vector Laboratories, UK) and were examined under a fluorescence microscope (Olympus BX 60). Images were captured at 20 _ magnification with an Evolution™ QE digital camera.

Following transwell co-culture as described above, DRG neu-rons were stained for the neuronal cytoskeletal marker BIII-tubulin (antibody diluted 1:500, mouse monoclonal, Sigma). After overnight incubation and PBS washes as above, the neurons were incubated with secondary antibodies (FITC-conjugated horse anti-mouse, diluted 1:100, Vector Laboratories, UK). Neur-ite outgrowth from the neuronal cells was assessed in 15 random fields and the length of the longest neurite was calculated by tracing its length from the most distal point back to the cell body using the ImageJ programme (http://rsbweb.nih.gov/ij/). For each type of co-culture a minimum of 100 neurons were counted. Analysis was carried out using GraphPad Prism 4 software (GraphPad, California, USA) and statistical significance tested using one-way ANOVA followed by Bonferroni post-testing.

Mitochondrial staining

The uMSC, dMSC, uASC and dASC (from neonatal and old rats) were stained with MitoTracker^S (MtT) Red

(M7512, CMXRos, Invitrogen) and BIII-tubulin (diluted 1:2000 rabbit polyclonal, Abcam, UK). The cells were plated at a density of 1 _ 10^4 in a chamber-slide flask and grown for 24 h. The cells were then washed with sterile PBS and the medium replaced with 1 mL of MtT solution (2% BSAþMtT Red, diluted 1:20 000) and incubated for 20 min at room temperature. The cells were then washed twice using sterile PBS and incubated with 4% (w/v) PFA/PBS solution for 30 min at RT. Finally, they were immunostained for BIII-tubulin as described above.

Transmission electron microscopy

Samples of SC, uMSC and uASC from young and old animals were cultured on 75 cm^2 flasks (Corning) and when they reached the confluence they were fixed in a solution of 2.5% (w/v) purified glutaraldehyde (Sigma, UK) and 0.5% (w/v) sucrose (Merck, Darmstadt, Germany) in 0.1 M So¨rensen phosphate buffer 7.4, for 6–8 h, then washed and stored in 0.1 M So¨rensen phosphate buffer with addition of 1.5% sucrose at 4–6 1C prior to embed-ding. Before embedding, the samples were washed for few minutes in So¨rensen phosphate buffer and then immersed for 2 h in 2% (w/v) osmium tetroxide (Sigma) in the same buffer solution. The samples were carefully dehydrated through graded alcohol with at least five passages of 5 min each. After two passages (7 min each) in propylene oxide (Sigma) and 2 h in a 1:1 mixture of propylene oxide and Glauerts' mixture of resins, the cells were embedded in Glauerts' mixture of resins, which comprises equal parts of Araldite M and the Araldite Harter, HY 964 (Merck) with the addition of plasticizer (0.5% w/v of dibutylphthalate) that promote the polymerisation of the embedding mixture. For the final step, a 2% accelerator 964, DY 064 (Merck) was added. Thin sections of the samples were cut in a thickness range of 50–70 nm with an ultramicrotome (Ultracut UCT, Leica Microsystems). Sections were collected and placed on grids previously coated with pioloform film. For transmission electron microscopy, grids were stained with uranyl acetate (saturated solution) for 15 min and lead citrate for 7 min, then washed and dried.

Statistical analysis

GraphPad Prism 4[&] software (GraphPad Software, San Diego, *CA*, USA) was used for statistical analysis of data. Following the various analytical methods, one-way ANOVA test followed by Bonferroni's Multiple Comparison test was used to determine differences between cell types originating from animals of different ages. All data were expressed as mean7SEM, and a value of at least *P*O0.05 was considered to be statistically significant.

Results

Quantification of Stro1 positive cells

To assess the proportion of undifferentiated stem cells in the cultures, cell counts were performed to determine the proportion of Stro1 positive cells as identified by immunocytochemistry staining of uASC and uMSC (Table 1). The percentage of stem cells identified by this marker cells is higher in the cultures from neonatal and young rats compare to those of the old group; similar results are obtained with both uASC and uMSC. Although the number of Stro1 positive cells decreased with increasing age of the animal, there was no statistical difference between the age groups within each cell type.

Proliferation assay

At each passage stage, SC, uMSC, dMSC, uASC and dASC from rats of different ages were kept proliferating for 10 days, but the proliferation assay reported here was measured at day 7 before full confluence of the cell cultures.

Table 1 – Number of Stro1 positive cells in cultures of undifferentiated adipose derived stem cells (uASC) and undifferentiated mesenchymal stem cell (uMSC) obtained from neonatal, young and old rats. The proportion of Stro-1 positive cells in calculated relative to the number of all cells in culture as identified by nuclear DAPI staining. Values are expressed as mean7SEM.

	DAPI positive cells	Stro1 positive cells	% Stro1 positive cells
uASC			
Neonatal	136711.53	8771	64.30
Young	166713.65	9274.51	55.84
Old	176739.89	89.3733.23	49.42
uMSC			
Neonatal	97.6726.73	68.6713.05	71.69
Young	146743.97	72.674.62	52.09
Old	160717.69	78.375.69	49.10

For neonatal SC, the proliferation rate tended to increase with the number of passages, but this increase was not statistically significant (Fig. 1A). The proliferation of the young SC was statistically significantly less between P1 *vs* P10 (*p*O0.05), P15 (*p*O0.01), P20 (*p*O0.001) and also between P5 *vs* P20 (*p*O0.001). Overall, the results indicated a tendency of decreasing prolifera-tion rate with increasing passage number (Fig. 1A). Similarly, in SC from old rats, the proliferation rate was decreased with an increasing number of passages; there was a statistically signifi-cant difference when comparing P1 *vs* P20 (*p*O0.05).

The proliferation rates of neonatal, young and old uASC were similar at different passages within each group, and there were no statistically significant differences between the different passages or age groups (Fig. 1B). Similarly, the results of the proliferation rate of neonatal, young and old dASC were compar-able between age groups. Although there was an increasing proliferation rate with increasing passage number in each age group, there were no statistically significant differences for the neonatal and young dASC (Fig. 1C). In contrast, the old dASC showed a significant (*p*O0.05) increase in the proliferation rate when P1 and P20 were compared (Fig. 1C).

The proliferation rate of the uMSC from neonatal, young and old rats was fairly constant with no statistical differences within each age group up to P15 (Fig. 1D); after this point, neonatal uMSC showed an increased proliferation rate compared to the young uMSC, and there were statistically significant differences between the two age groups at P20 (*p*O0.01) (Fig. 1D). The proliferation rate of the old uMSC showed a tendency to decrease with increasing number of passages, and there was a statistical significance when P1 *vs* P20 (*p*O0.05) were compared. The proliferation rate of dMSC from neonatal, young and old rats showed a similar pattern and there were no statistically sig-nificant differences between the proliferation rates with number of passages or between age groups (Fig. 1E).

Notch-2 receptor gene expression

RT-PCR analysis showed that undifferentiated and differentiated ASC and MSC from animals of all ages expressed Notch-2 mRNA at a similar level (Fig. 2). Also, all of these cells appear to express the Notch-2 receptor gene at a similar level to that of SC from animals of comparable age.

Expression of p38 protein

Western blot analysis of p38 expression showed that the protein was present in all the groups of cells and its expression appeared to increase with the aging of the rats (Fig. 3A). Densitometric analysis showed that there was no significant difference in p38 protein levels between the neonatal, young and old SC (Fig. 3B). In the uASC group the expression of p38 increased with increasing animal age and there was a statistically significant difference (*p*O0.01) in its expression when comparing neonatal and old uASC (Fig. 3C). Interestingly, this increase was also seen in the dASC cells, with a statistically significant difference (*p*O0.05) between the neonatal dASC and old dASC (Fig. 3D). The results showed a similar pattern of p38 expression for ASC from different age groups whether undifferen-tiated or differentiated. In contrast, the undifferentiated MSC from neonatal, young and old rats showed a similar expression level of p38 (Fig. 3E) with no statistically significant difference between groups. Similarly, there were no detectable changes in p38 expres-sion in dMSC from neonatal, young and old animals (Fig. 3F).

Expression of p53 protein

Densitometric analysis of western blots for p53 protein (Fig. 4A) in SC, uASC, dASC uMSC and dMSC from the three age groups of animals showed there was a progressive increase of p53 levels with increase in animal age (Fig. 4B–F). For the majority of cell types this increase was not statistically significant, except for dASC where there were significant differences in p53 levels in cells of neonatal *vs* young (*p*O0.01), young *vs* old (*p*O0.01) and neonatal *vs* old (*p*O0.001) rats.

DRG neuron co-cultures

Immunocytochemical staining for BIII tubulin was used to show the extent of neurite outgrowth from dissociated DRG neurons (from adult rats) co-cultured with SC or differentiated ASC and MSC from rats of different ages. Previously, we demonstrated that the neurite outgrowth is related to the presence of stem cells [2] and to the level of growth factors secreted by SC or differentiated stem cells [4]. This was confirmed by the negative results of the control experiments we carried out where dASC, dMSC or SC were omitted from the insert (results not shown). In co-culture with neonatal cells, the DRG neurite outgrowth was similar for the three types of cells although the length of neurites obtained in co-culture with dMSC was slightly lower, but not statistically significantly so compared to the values obtained with the other two cell types (Fig. 5A). When using cells from young animals (Fig. 5B), there was a significant increase in neurite length when the neurons were co-cultured with dMSC compared to co-culture with SC and dASC (*p*O0.001). There was no significant difference in neurite lengths between co-cultures with SC or dASC. The DRG were also responsive to co-culture with old SC, dASC and dMSC. The neurite length quantification showed a significantly longer neurite length when DRG were stimulated by old dASC (*p*O0.001) and dMSC (*p*O0.001) compared to old SC. There was no significant difference in the length of neurites seen in co-cultures of neurons with old dASC and dMSC (Fig. 5C).

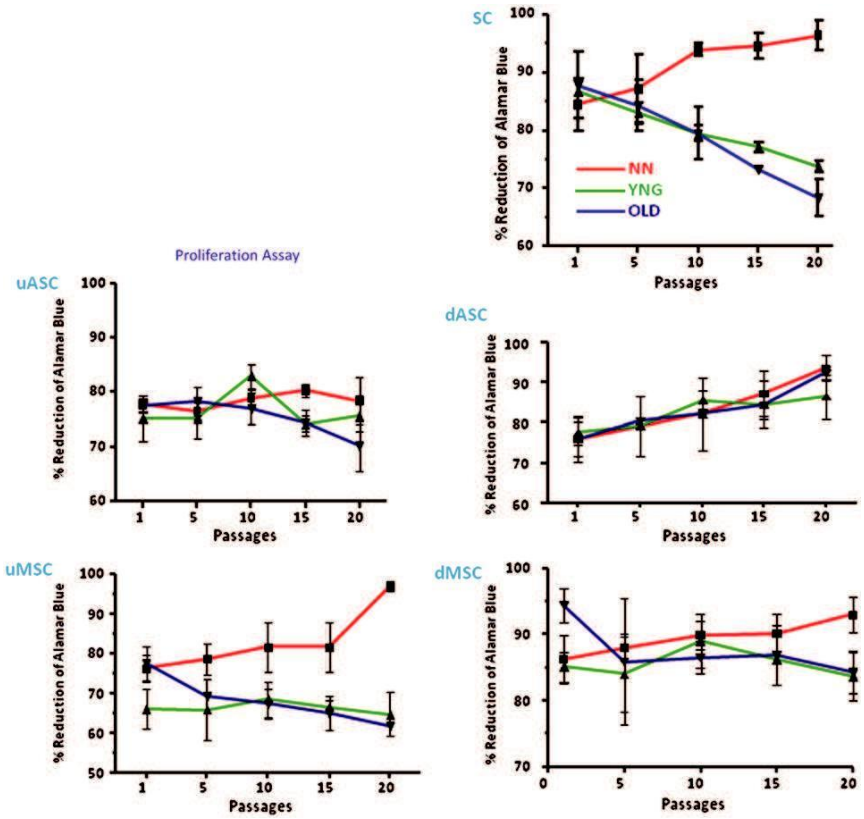

Fig. 1 – Proliferation rates of SC, uASC, dASC, uMSC and dMSC from neonatal (NN), young (YNG) and old (OLD) animals at passages 1, 5, 10, 15 and 20. SC: In the neonatal SC group, there were no significant differences in proliferation rate between any of the passages. In young SC, there were differences between P1 VS P10 (PO0.05), P1 VS P15 (PO0.01), P1 VS P20 (PO0.001) and P5 VS P20 (PO0.01). In the old SC, the proliferation rate decreased as passage number increased, reaching a significant difference at P20 compared to P1 (PO0.05).

ASC: In neonatal, young and old uASC the proliferation rates were similar with no significant differences between any of the passages. In neonatal and young dASC groups there were no significant differences in proliferations rates between any of the passages. In the old dASC, the proliferation rate gradually increased with increasing passage number, with a significant difference between P20 and P1 (PO0.05). MSC: In the neonatal uMSC and young uMSC group, the proliferation rate of the cells was comparable between P1 and P15, but a significant difference was seen between P1 and P20 (PO0.01). In old uMSC, the proliferation rate was similar in the early passages, but decreased significantly at P20 compared to P1 (PO0.05). In neonatal, young and old dMSC, the cell growth was similar and there were no significant differences in proliferation rate between any of the passages. Values are expressed as mean7SEM.

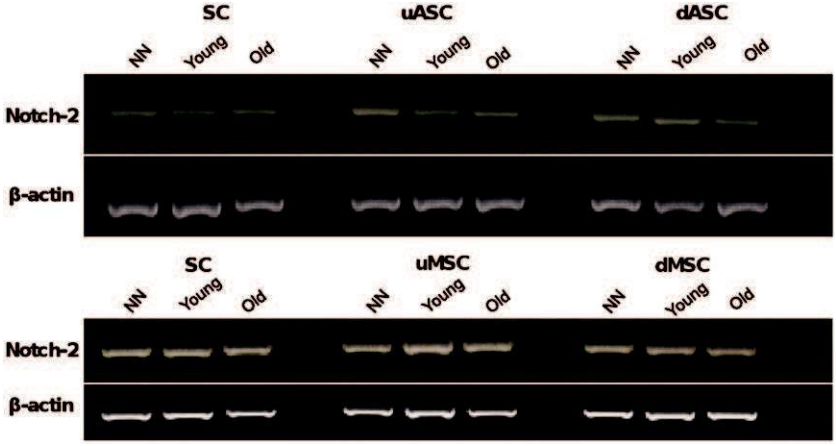

Fig. 2 – RT-PCR analysis of Notch-2 receptor mRNA expression in SC, undifferentiated and differentiated ASC (uASC and dASC), undifferentiated and differentiated MSC (uMSC and dMSC) from neonatal (NN), young (YNG) and old rats. The Notch-2 transcript was present in all the cell types and at similar levels. The B-actin transcript was used as a control for amplification efficacy and gel loading.

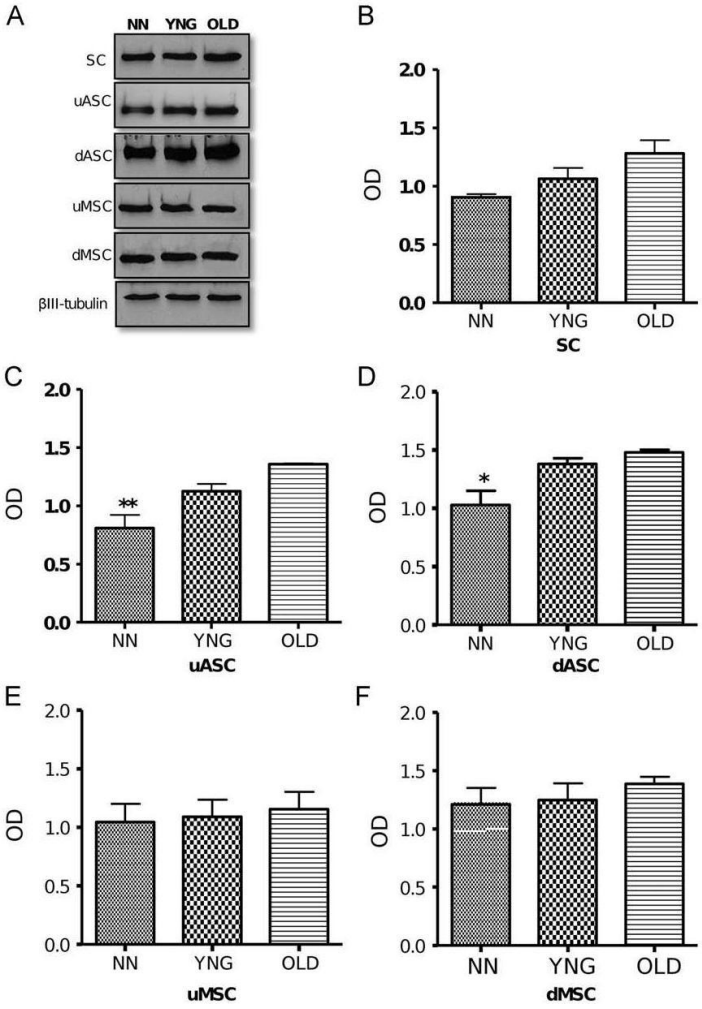

Fig. 3 – (A) Western blotting detection of protein p38 in whole cells lysates of cultured SC, undifferentiated and differentiated MSC and ASC from rats of different ages. A higher level of p38 protein was seen in all cell types in the old rat group compared to the neonatal group. (B–F) Densitometric analysis of p38 expression in SC, uMSC, dMSC, uASC and dASC from neonatal (NN), young (YNG) and old (OLD) rats. OD values are expressed as the ratio of p38 band density to that of corresponding BIII-tubulin (loading control) band. There was a statistically significant difference between neonatal VS old in uASC (PO0.001) (C) and in dASC (PO0.05)

(D). There were no statistically significant differences in p38 expression between neonatal, young and old for SC (B) uMSC (E) and dMSC (F). Values are expressed as mean7SEM.

Mitotracker^{S} staining of mitochondria

Mitotracker^{S} Red staining was carried out to determine the distribution pattern of mitochondria, which indicates their fission or fusion state, within the SC, uMSC, dMSC, uASC and dASC. Cells from only the neonatal and old rats were assessed for mitochondrial distribution pattern because cells from these age groups were more likely to present discernable differences. In neonatal SC (Fig. 6A), uASC (Fig. 7A) and uMSC (Fig. 8A) mitochondria were distributed throughout the cytoplasm and showed a linear distribution (fusion) typical of healthy cells. In appeared fragmented in the cytoplasm and localised around the nucleus as seen in old SC (Fig. 6C), which may indicate a possible pro-apoptotic stage of the cells during aging.

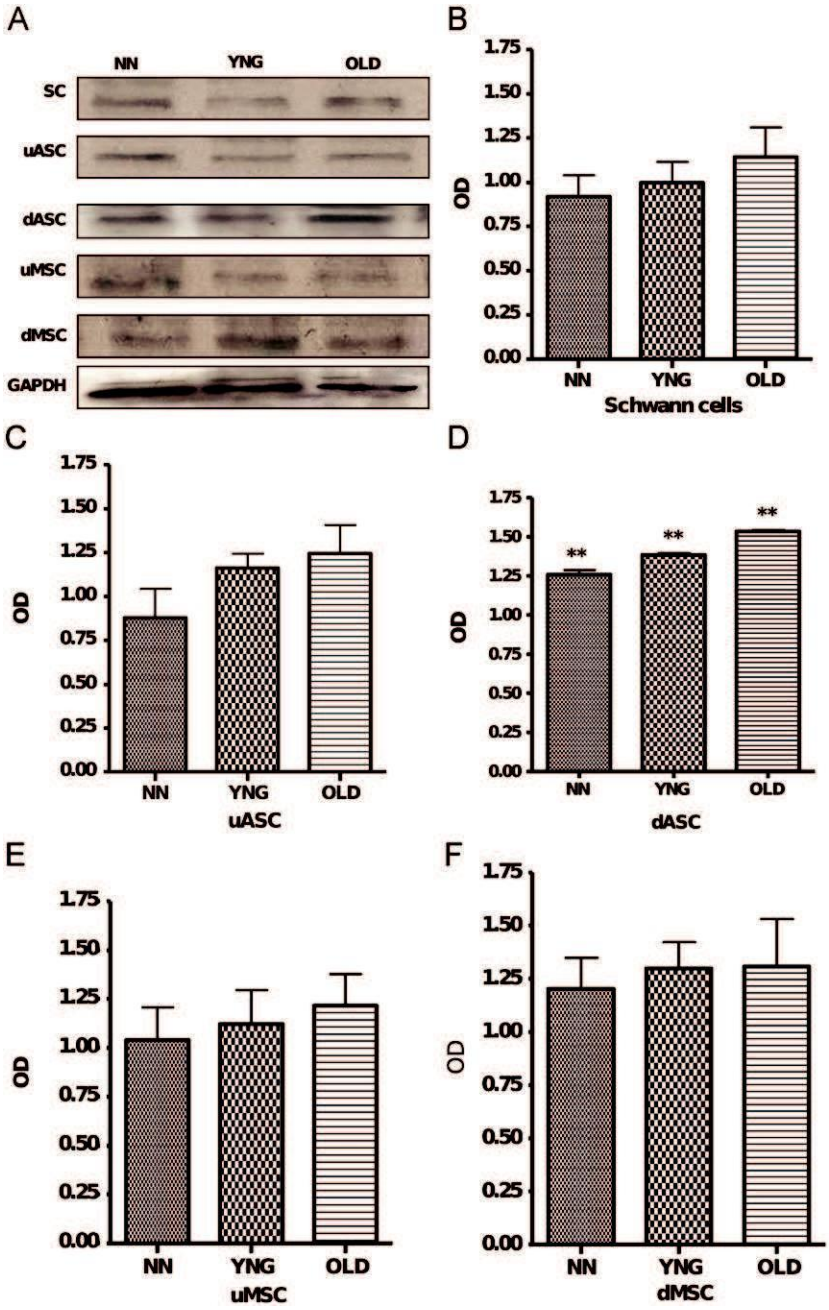

Fig. 4 – (A) Western blotting and (B–F) densitometric analysis of p53 expression in SC, uASC, dASC, uMSC and dMSC isolated from neonatal (NN), young (YNG) and old (OLD) rats. Protein p53 quantification OD values are expressed as a ratio of p53 band density to that of the corresponding GAPDH (loading control) band. The p53 levels in SC (B) uASC (C), uMSC (E) and dMSC cells (F) increased with age, but with no statistically significant differences between neonatal, young and old rats. In dASC (D), there were significant differences in p53 levels in neonatal VS young (PO0.01) and young VS old (PO0.01) and neonatal VS old (PO0.001) cells. Values are expressed as mean7SEM.

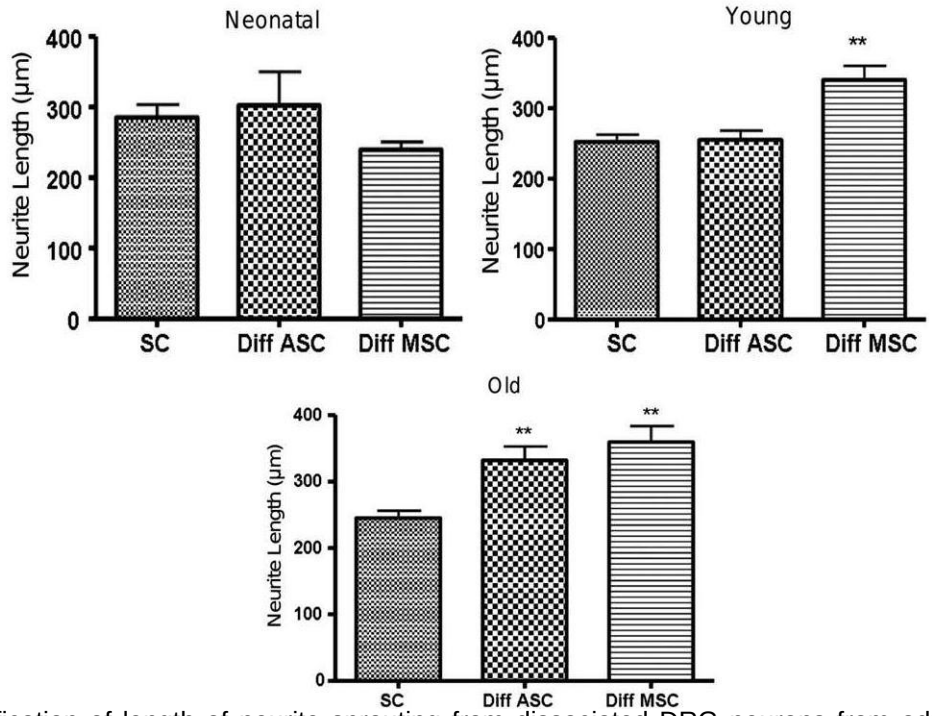

Fig. 5 – Quantification of length of neurite sprouting from dissociated DRG neurons from adult rats following non-contact co-culture for 24 h with SC, dASC or dMSC from rats of different ages. In the neonatal rat group, there were no significant differences in neurite outgrowth lengths between cell types. In the young animal group, there was no statistical difference between SC and dASC, but there were differences in neurite length between dMSC VS SC and dASC (PO0.001). In the old rat group, there was a statistic difference in between dASC VS SC (PO0.001) and dMSC VS SC (PO0.001). Values are expressed as mean neurite length (Lm)7SEM.

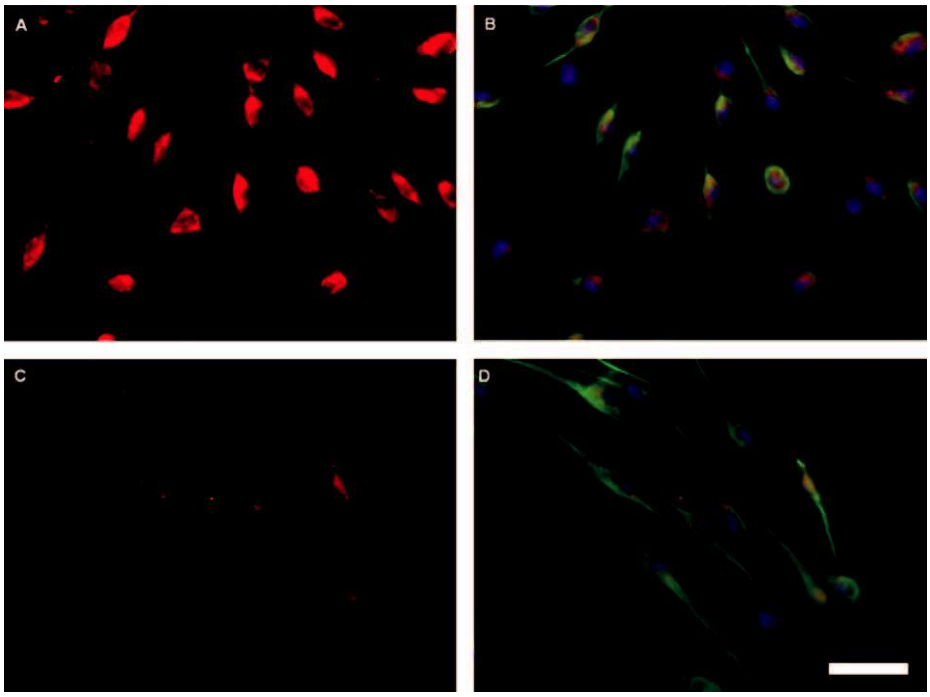

Fig. 6 – Cultured SC from neonatal (A and B) and old rats (C and D) stained for mitochondria (Mitotracker^{S}-Red) (A and C) and BIII-tubulin (FITC: green, DAPI: blue) (B and D). Magnification _ 40, scale bar¼50 Lm. (For interpretation of the references to color in this figure legend, the reader is referred to the web version of this article.)

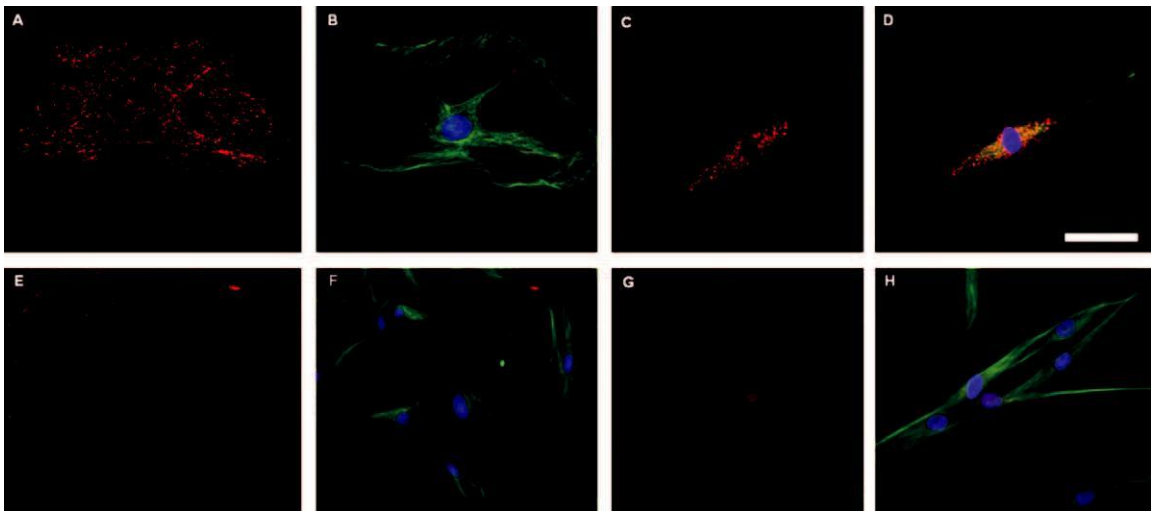

Fig. 7 – uASC (A, B, E, F) and dASC (C, D, G, H) from neonatal (A–D) and old rats (E–H) stained for mitochondria (Mitotracker^{S}-Red) (A, C, E, G) and BIII-tubulin (FITC: green, DAPI: blue) (B, D, F, H). Magnification _ 40, scale bar¼50 Lm. (For interpretation of the references to color in this figure legend, the reader is referred to the web version of this article.)

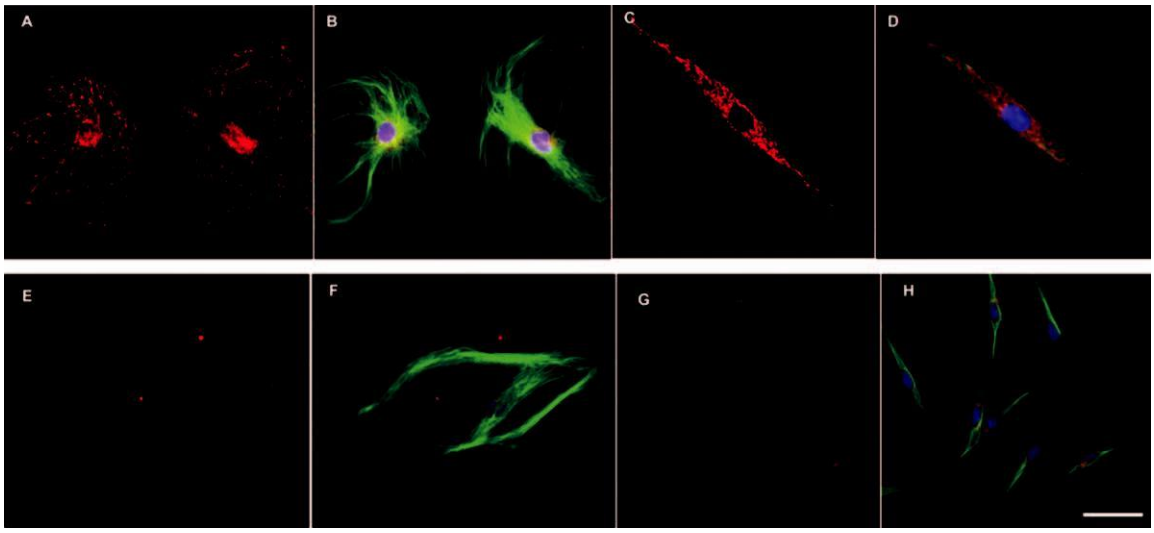

Fig. 8 – uMSC (A, B, E, F) and dMSC (C, D, G, H) from neonatal (A–D) and old rats (E–H) stained for mitochondria (Mitotracker^{S}-Red) (A, C, E, G) and BIII-tubulin (FITC: green, DAPI: blue) (B, D, F, H). Magnification _ 40, scale bar¼50 Lm. (For interpretation of the references to color in this figure legend, the reader is referred to the web version of this article.)

Electron microscopy cell morphology

SC of young and old rats appeared very different in their ultra-structural morphology. Young SC displayed a rounded and euchro-matic nucleus, usually with no nucleolus (Fig. 9A), and a cytoplasm rich in mitochondria and small isolated elements of the rough endoplasmic reticulum (Fig. 9B). In contrast, the old cells had a lobular and heterochromatic nucleus (Fig. 9C) surrounded by a dense, less organised cytoplasm with few organelles, many vacuoles and disrupted mitochondria structure (Fig. 9D). In the cells from old animals the membrane showed a greater number of pseudopodia

(Fig. 9C) compared to the membrane structure of the young SC. Stem cells isolated from adipose tissue of young rats exhibited an eccentric and lobed nucleus, with one or more nucleoli (Fig. 10A). The nucleus showed mainly euchromatin with a heterochromatin layer distrib-uted along the inner side of nuclear membrane. In these cells, the cytoplasm appeared abundantly rich in organelles, mitochondria and endoplasmic reticulum (Fig. 10B). The plasma membrane of young cells was irregular with pseudopodia, which is indicative of a great capacity for adhesion and migration (Fig. 10A). In the old ASC, the pseudopodia were less evident and the membrane was more pronounced and regular, while that of the nucleus was irregular (Fig. 10C). The cytoplasm of old ASC showed abundant vacuoles containing fat, a typical characteristic of senescent cells (Fig. 10D), and abnormal mitochondria structure. MSC from young and old rats showed similar characteristics to ASC cells. Young MSC displayed a large pale lobular nucleus with a large amount of euchromatin and conspicuous nucleoli (Fig. 11A). Dilated cisterns of rough endoplas-mic reticulum were present in cytoplasm with a well organised mitochondrial structure (Fig. 11B). The old MSC displayed an irregular shaped nucleus with a disorganised cytoplasm and mito-chondria with thin cristae and evident signs of ultrastructural disruption (Fig. 11D).

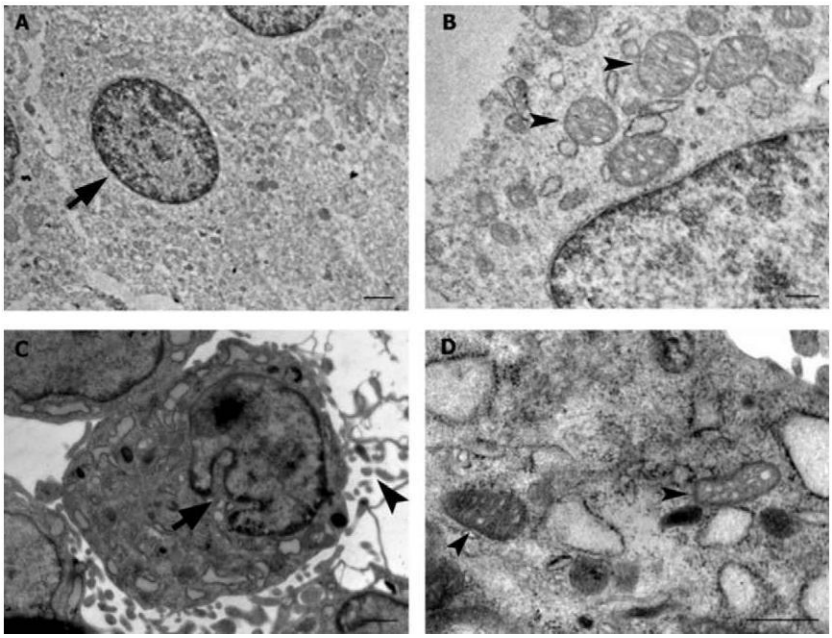

Fig. 9 – Representative electron micrographs of SC from young (A, B) and old (C, D) animals. The nucleus in the young cells (arrow, A) is regular and without a nucleolus, while that of old cells shows a lobular appearance (arrow, C) and numerous membrane pseudopodia (arrowhead, C). The mitochondria are numerous in the young cells (arrowhead, B), while they are more sparse in the old cells, at time showing disrupted morphology (arrowhead, D). Scale bars: (A and C) 1 Lm; (B and D) 0.5 Lm.

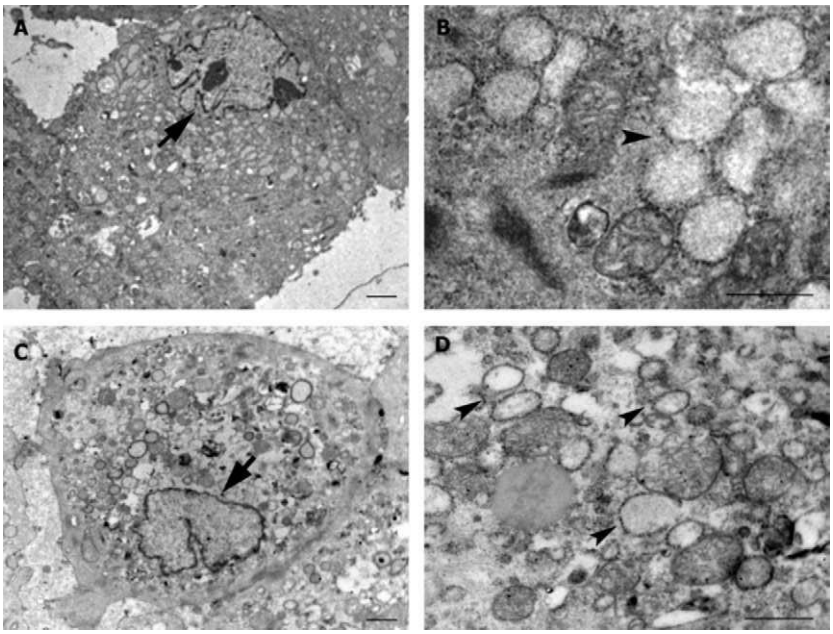

Fig. 10 – Representative electron micrographs of uASC from young (A, B) and old animals (C, D). The young cells show a lobed nucleus (arrow, A) and a rich endoplasmic reticulum (arrowhead, B). In contrast, the nucleus in the old cells is irregular (arrow, C), and the cytoplasm shows abundant vacuoles containing fat (arrowhead, D). Scale bars: (A and C) 2 Lm; (B and D) 0.5 Lm.

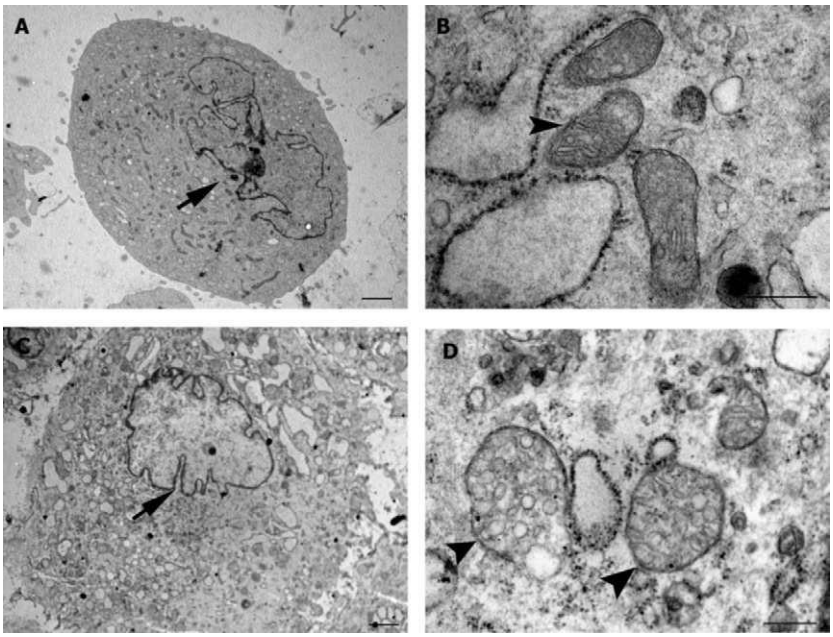

Fig. 11 – Representative electron micrographs of uMSC from young (A, B) and old animals (C, D). As seen in ASC, the young cells show a lobed nucleus (arrow, A) and regularly structured mitochondria (arrowhead, B). In the old cells, the nucleus is irregular (arrow, C) and the mitochondria show evident signs of degeneration (arrowheads, D). Scale bars: (A and C) 1 Lm; (B and D) 0.2 Lm.

Discussion

Adult stem cells have been shown to be capable of differentiation into various lineages. Due to many promising applications of tissue engineering that require cell expansion following harvest, the effect of donor age and the IN VITRO handling require investigation in order to avoid pitfalls in the development of cell based therapies. In this study, SC, MSC and ASC isolated from sciatic nerve, bone marrow and adipose tissue, respectively, from neonatal, young (four months) or old (twenty months) rats were compared in terms of their IN VITRO growth

kinetics, expression of senescence proteins and morphological structure to investigate whether the aging of the cells or number of passages might influence their functionality.

Stro1 was used as a marker of undifferentiated stem cells in preference to other markers as it recognises non-haematopoietic progenitor cell with a stable undifferentiated phenotype [35]. Also, we previously found that expression of other markers is inconsistent. Alkaline phosphatase, which should decline only with differentiation, was found to decrease progressively with the number of passages, while nestin expression was variable in undifferentiated stem cells [2,3]. Furthermore, studies on osteo-genic stem cells [36] and muscle precursor cells [25] indicated that Stro1 is present in rats of all ages. Quantification of the stem cell surface marker Stro1 confirmed that for both MSC and ASC the percentage of Stro1 positive cells was similar for neonates and young adults, but with a decrease in Stro1 positive cells from old animals. These data would indicate that there is a limited decline in the number of stem cells harvested from bone marrow or fat with increasing age of the donor.

A proliferation assay was used to compare the growth char-acteristics of the stem cells for up to twenty passages. The Alamar Blue assay was chosen as it allows repeated measure-ment of cell proliferation without destruction of the cultures, and it gives proliferation measurements equivalent to those carried out with BrdU incorporation [37,38]. In neonatal SC the number of passages does not appear to negatively influence the growth rate of the cells. However, SC from both young and old animals showed a decline in proliferation with the increasing passage number. In old SC, the difference between the initial and the final passages, P1 and P20, respectively, was particularly evident and may be indicative of cell senescence over time. Generally, in the uASC and dASC groups the growth curve is similar among the different age groups, although the old dASC showed a more marked proliferation increase over time. Neonatal uMSC showed an increased proliferation during the later passages, while old uMSC showed a slow but constant decline of proliferation over time. The proliferation rate of dMSC varied little over time and was comparable for the cells from the different age groups.

The uMSC and uASC from old rats showed similar decreases in proliferation rate with increase in passage number (P20). Although the number of passages investigated here is not sufficient to fully reflect the IN VIVO aging process, the uMSC and uASC from old rats showed initial signs of age-related senescence. These signs of proliferative senescence were consistent with the morphological changes found by electron microscopy. However, following differ-entiation this decline in proliferation rate appears to be reversed as there were no major differences in the growth curves between the three age groups. Moreover, there was a significant increase in proliferation rate with number of passages observed for dASC. A possible explanation for this observation could be the influence of the growth factors used for the IN VITRO differentiation process. Indeed, restoration of mitogenic and growth signalling may rejuve-nate cells, and instead of entering in a senescence cycle the cells respond to growth factor induced ‘reprogramming’ that leads them to maintained proliferation despite the high passage number [13]. The results of recent studies showed that MSC harvested from donor animals of different ages and cultured for different numbers of passages showed a decrease in their chondrogenic and osteogenic potential with increasing passage number, whereas their adipogenic potential decrease with donor age [39]. Conversely, others have shown that there were no age related differences in rat MSC differentiation or changes in proliferation, attachment and senes-cence [10,11,40,41].

It has been shown that Notch gene signalling regulates differentia-tion and maintenance of stem cells, while Notch-1 activation promotes stem cell self-renewal [42]. In this study, Notch-2 was preferentially chosen as it was shown previously to govern the repopulation of murine stem cells [43]. Notch-2 signalling also enhanced the self-renewal of haematopoietic stem cells by prevent-ing depletion, which might result from environmental factors such as stress-induced stimuli [44]. Here we have shown that Notch-2 gene expression is similar in all cell types at all ages, a result which is consistent with generally consistent proliferation rates of all cells with increased passages, and with a limited decrease of Stro1 positive stem cells with increased donor age.

The p38 MAP kinase pathway is activated in response to physical stress signals, such as osmotic shock, heat, UV light, and in response to pro-inflammatory cytokines, such as TNF-A, IL-1 and growth factors, for example bFGF and PDGF [40]. In this study, the expression of p38 protein was detected in the different cell types isolated from animals of all ages. Quantification of p38 protein expression showed there to be a slight upward trend in expression level with increasing age of the donor animal. While in the groups of SC and MSC (undifferentiated and differentiated) the increase in expression of p38 was not statistically significant, in the

uASC and the dASC groups the expression of p38 was more evident and was statistically significant in cells from old rats. This result could be a further indication that the cellular senescence may be linked to the age of the donor. In the dASC there are significant differences in p38 expression levels when neonatal rat cells are compared to young and old rat cells, but the difference is not significant when comparing the young to the old group. Although in the group of uASC the difference could be attribute mainly to the age of donor, in the dASC it could be hypothesised that an involvement of growth factors, such as the FGF2 and PDGF used for the differentiation and maintenance of the stem cells, could affect the expression of the p38 and consequently cell proliferation [40]. Indeed, p38 has been impli-cated in cell cycle arrest, DNA repair and programmed cell death [45–47]; its activation has also been associated with the cellular response to stress rather than proliferation [45–48].

The protein p53 regulates cell cycle progression and apoptosis, but it can also directly modulate the transcription of genes that are specifically required for neuronal differentiation [49,50]. The function of p53 in development and its importance in the control of differentiation processes have been previously established with some discrepancies; some studies suggest that p53 facil-itates cell differentiation whereas in others it seems to be suppressive [51,52]. Our study showed that the expression of p53 protein in all cell types (SC, uMSC, dMSC, uASC and dASC) from the three different age donors did not differ significantly. The level of the expression of p53 protein appears to be slightly increased in both differentiated ASC and MSC compared to the undifferentiated cells. Mutations in p53 have been implicated in age-related mesenchymal stem cell transformation and in the self-renewal and differentiation of neural stem cells [53,54]. The activity of p53 protein was initially thought to be limited to the nucleus, although recently it became apparent that p53 also regulates mitochondrial response to stress stimuli [55,56]. More-over, it was demonstrated that p53 might also regulate the aging process and this pro-aging activity is thought to result from chronic p53-dependent apoptosis and senescence, resulting in cancer resistance at the expense of tissue atrophy [57]. Further investigation showed that p53 protein might promote or retard aging by altering the systemic or local tissue milieu through the activation of the IGF-I signalling pathway and the senescence-associated secretory phenotype (SASP) [58]. However, from the results we obtained, p53 does not appear to significantly influence the biology of Schwann or stem cells.

In this study, adult DRG neuron co-cultures were used to assess neurite outgrowth as indicative of growth factor secretion by ASC and MSC following their differentiation into SC-like cells [4]. Indeed, untreated DRG neurons in culture fail to extend neurites unless influenced by trophic factors [4]. Previous studies have shown that the DRG neurons are able to extend neurites in the absence of exogenous NGF, an effect due to soluble factors release by the cells in non-contact co-culture [2]. Moreover, secretion of BDNF and NGF was not found from undifferentiated stem cells, but it was due to their differentiation to the glial cell lineage [4]. Consistently, the indirect co-culture system used in this study has shown that growth factors secreted by SC and differentiated MSC and ASC from animals of all ages elicited neurite outgrowth. There were no significant differences in the DRG neurite lengths following co-culture with neonatal SC, dASC and dMSC. Similar results were obtained with co-cultures of SC and dASC from young animals, but, in contrast, dMSC from young rats appeared to stimulate more neurites growth compared to dASC and SC. There is a statistically significant increase in the length of neurites in the co-cultures of DRG neurons with dASC or dMSC derived from old rats compared to those with SC from animals of the same age. It is well known that nerve regeneration is dependent on a secretion of growth factors from glial cells [1], and these results indicate that differentiated stem cells from older individual can promote nerve regeneration. The discrepancy between the results of DRG neuron co-cultures with neonatal cells and old cells is notable and unexpected. Increased expression of p53 in differentiated stem cells may be indicative of an increase in cellular senescence and therefore to their reduced functionality. However, it has also been shown that cellular senescence, as defined by the loss of proliferative potential, is linked to cellular over-activation and correlates with cellular hypertrophy [59]. In the case of differentiated stem cells, this over activation might correlate with the increase in growth factor secretion and consequently the increased stimulation of neurite outgrowth.

Degenerative events such as oxidative stress, exposure to UV light and aging culminate in the loss of cell functionality, and mitochon-drial dysfunction in aged stem cells, which may be an indicative sign of impending cell death. This study focused on investigating both the intra-cellular distribution and gross morphology of the mitochondria in cells derived from neonatal and old animals. Mitotracker^{S} staining of mitochondria reveals their dynamic morphology, which changes to meet the metabolic needs of the cell, an event that is regulated by two main processes, mitochondrial fission and fusion [60]. In mammalian cells, the mitochondrial population aligns in strategic subcellular positions to form long, interconnected networks by mitochondrial fusion. Conversely, in pre-apoptotic cells the mito-chondria appear as short unconnected units, a state defined as mitochondria fission. A firm link between mitochondrial dynamics and cell function has yet to be established, but recent investigation on Drp1 null mutants provides a link between mitochondrial fragmentation and apoptosis. Drp1 null mice are incapable of initiating mitochondrial fission, and important apoptotic-related events, such as cytochrome C release, are blocked and neuronal death is strongly inhibited [61]. Fragmentation of mitochondria during cell death has been shown to play a key role in cell death progression, including the release of mitochondrial apoptotic pro-teins [30]. Ultrastructural changes in mitochondria, such as cristae remodelling, are also involved in cell death initiation and are initial sign of senescence [62]. In our study mitochondrial changes in cells from animals of different ages were evident as shown by both Mitotracker^{S} staining and electron microscopical analysis. Unlike neonatal cells, SC, ASC and MSC from old rats showed distinct changes structural with mitochondria clustered around the nucleus, which would indicate a reduction of fusion and increased fission as seen in pre-apoptotic cells. The aggregation of mitochondria in the perinuclear area of the cells may occur for a variety of reasons. In the main, mitochondria in mammalian cells are moved around along microtubules [63], and disruption of fission protein Drp1 results in perinuclear clustering of mitochondria [63,64]. Perinuclear clustering of mitochondria has also been observed in apoptosis in necrosis [65]. Furthermore, electron microscopical studies of SC, ASC and MSC showed mitochondrial degeneration and loss of the cristae indicating a reduced amount of available inner mitochondrial membrane in the old animal cells. A diminished expression of respiratory chain complexes could be a consequence of these structural changes, resulting in a reduced membrane potential [66]. Taken together, the reduced mitochondrial fusion and their perinuclear clustering might indicate decreased energy production in ageing cells.

Conclusions

The results of this study show that the cells from aged animals expressed markers such as p38 and p53 which are typical of senescence, and that the intensity of the staining of the mitochondria was decreased possibly due to a reduction in mitochondria activity. However, these features do not seem to affect the cell proliferation rate or their growth factor secreting function, as indicated by the neurite outgrowth from DRG neurons in non-contact co-cultures. Other studies have shown that age does not affect the ability of MSC and ASC to support the regeneration process following injury [67,68], which are consistent with our results showing that MSC and ASC from aged rats differentiated into SC-like retain the potential to support axon regeneration. The increased understanding of the biological mechanisms of MSC and ASC derived from donors of different ages will expand their functional applications in tissue engineering and maximise their therapeutic use.

Acknowledgments

The authors are grateful for the generous financial support of the Rosetrees Trust, the Swedish Medical Research Council, (EU), the County of Vasterbotten, the Aner Foundation, the British Council/ CRUI (British-Italian Partnership Programme for Young Researchers) and the Regione Piemonte (Progetto Ricerca Sanitaria Finalizzata). The authors also wish to thank Acorda Therapeutics for their generous gift of GGF-2.

REFERENCES

[1] G. Terenghi, Peripheral nerve regeneration and neurotrophic factors, J. Anat. 194 (1999) 1–14.

[2] J. Caddick, P.J. Kingham, N.J. Gardiner, M. Wiberg, G. Terenghi, Phenotypic and functional characteristics of mesenchymal stem cells differentiated along a Schwann cell lineage, Glia 54 (2006) 840–849.

[3] P.J. Kingham, D.F. Kalbermatten, D. Mahay, S.J. Armstrong, M. Wiberg, G. Terenghi, Adipose-derived stem cells differentiate into a Schwann cell phenotype and promote neurite outgrowth IN VITRO, Exp. Neurol. 207 (2007) 267–274.

[4] D. Mahay, G. Terenghi, S.G. Shawcross, Growth factors in mesenchymal stem cells following glial-cell differentiation, Biotechnol. Appl. Biochem. 51 (2008) 167–176.

[5] M. Brohlin, D. Mahay, L.N. Novikov, G. Terenghi, M. Wiberg, S.G. Shawcross, L.N. Novikova, Characterisation of human mesench-ymal stem cells following differentiation into Schwann cell-like cells, Neurosci. Res. 64 (2009) 41–49.

[6] C. Mantovani, D. Mahay, P.J. Kingham, G. Terenghi, S.G. Shaw-cross, M. Wiberg, Bone marrow- and adipose-derived stem cells show expression of myelin mRNAs and proteins, Regen. Med. 5 (2010) 403–410.

[7] P.G. di Summa, D.F. Kalbermatten, E. Pralong, W. Raffoul, P.J. Kingham, G. Terenghi, Long-term IN VIVO regeneration of peripheral nerves through bioenegineered nerve grafts, Neuro-science 181 (2011) 278–291.

[8] A. Aguirre, M.E. Rubio, V. Gallo, Notch and EGFR pathway interaction regulates neural stem cell number and self-renewal, Nature 467 (2010) 323–327.

[9] S. Sethe, A. Scutt, A. Stolzing, Aging of mesenchymal stem cells, Ageing Res. Rev. 5 (2006) 91–116.

[10] C.G. Bellows, W. Pei, Y. Jia, J.N. Heersche, Proliferation, differ-entiation and self-renewal of osteoprogenitors in vertebral cell populations from aged and young female rats, Mech. Ageing Dev. 124 (2003) 747–757.

[11] S.V. Tokalov, S. Gruner, S. Schindler, G. Wolf, M. Baumann, N. Abolmaali, Age-related changes in the frequency of mesenchy-mal stem cells in the bone marrow of rats, Stem Cells Dev. 16 (2007) 439–446.

[12] V.D. Roobrouck, F. Ulloa-Montoya, C.M. Verfaillie, Self-renewal and differentiation capacity of young and aged stem cells, Exp. Cell Res. 314 (2008) 1937–1944.

[13] S.R. Mayack, J.L. Shadrach, F.S. Kim, A.J. Wagers, Systemic signals regulate ageing and rejuvenation of blood stem cell niches, Nature 463 (2010) 495–500.

[14] G. Li, C. Luna, P.B. Liton, I. Navarro, D.L. Epstein, P. Gonzalez, Sustained stress response after oxidative stress in trabecular meshwork cells, Mol. Vis. 13 (2007) 2282–2288.

[15] L. Hayflick, The limited IN VITRO lifetime of human diploid cell strains, Exp. Cell Res. 37 (1965) 614–636.

[16] E.A. Pollina, A. Brunet, Epigenetic regulation of aging stem cells, Oncogene 30 (2011) 3105–3126.

[17] T. Kuilman, C. Michaloglou, W.J. Mooi, D.S. Peeper, The essence of senescence, Genes Dev. 24 (2010) 2463–2479.

[18] D. De Paula, M.V. Bentley, R.I. Mahato, Effect of iNOS and NF-kappaB gene silencing on beta-cell survival and function, J. Drug Target 15 (2007) 358–369.

[19] K. Ito, A. Hirao, F. Arai, K. Takubo, S. Matsuoka, K. Miyamoto, M. Ohmura, K. Naka, K. Hosokawa, Y. Ikeda, T. Suda, Reactive oxygen species act through p38 MAPK to limit the lifespan of hematopoietic stem cells, Nature Med. 12 (2006) 446–451.

[20] E. Batchelor, A. Loewer, C. Mock, G. Lahav, Stimulus-dependent dynamics of p53 in single cells, Mol. Syst. Biol. 7 (2011) 488.

[21] Z.N. Demidenko, L.G. Korotchkinam, A.V. Gudkov, M.V. Blago-sklonny, Paradoxical suppression of cellular senescence by p53, Proc. Natl. Acad. Sci. USA 107 (2010) 9660–9664.

[22] L.G. Korotchkina, O.V. Leontieva, E.I. Bukreeva, Z.N. Demidenko, A.V. Gudkov, M.V. Blagosklonny, The choice between p53-induced senescence and quiescence is determined in part by the mTOR pathway, Aging (Albany NY) 2 (2010) 344–352.

[23] Z. Feng, W. Hu, A.K. Teresky, E. Hernando, C. Cordon-Cardo, A.J. Levine, Declining p53 function in the aging process: a possible mechanism for the increased tumor incidence in older popula-tions, Proc. Natl. Acad. Sci. USA 104 (2007) 16633–16638.

[24] D.J. Rossi, C.H. Jamieson, I.L. Weissman, Stems cells and the pathways to aging and cancer, Cell 132 (2008) 681–696.

[25] I.M. Conboy, M.J. Conboy, G.M. Smythe, T.A. Rando, Notch-mediated restoration of regenerative potential to aged muscle, Science 302 (2003) 1575–1577.

[26] A. Navarro, R. Torrejon, Role of nitric oxide on mitochondrial biogenesis during the ovarian cycle, Front. Biosci. 12 (2007) 1164–1173.

[27] R.J. Youle, M. Karbowski, Mitochondrial fission in apoptosis, Nat. Rev. Mol. Cell. Biol. 6 (2005) 657–663.

[28] D.C. Chan, Mitochondrial fusion and fission in mammals, Annu. Rev. Cell Dev. Biol. 22 (2006) 79–99.

[29] M.J. Barsoum, H. Yuan, A.A. Gerencser, G. Liot, Y. Kushnareva, S. Graber, I. Kovacs, W.D. Lee, J. Waggoner, J. Cui, A.D. White, B. Bossy, J.C. Martinou, R.J. Youle, S.A. Lipton, M.H. Ellisman, G.A. Perkins, E. Bossy-Wetzel, Nitric oxide-induced mitochondrial fission is regulated by dynamin-related GTPases in neuron, EMBO J. 25 (2006) 3900–3911.

[30] E.C. Cheung, H.M. McBride, R.S. Slack, Mitochondrial dynamics in the regulation of neuronal cell death, Apoptosis 12 (2007) 979–992.

[31] J. Rehman, Empowering self-renewal and differentiation: the role of mitochondria in stem cells, J. Mol. Med. (Berl.) 88 (2010) 981–986.

[32] H.M. McBride, M. Neuspiel, S. Wasiak, Mitochondria: more than just a powerhouse, Curr. Biol. 16 (2006) R551–R560.

[33] J. Yeon Lim, S.S. Jeun, K.J. Lee, J.H. Oh, S.M. Kim, S.I. Park, C.H. Jeong, S.G. Kang, Multiple stem cell traits of expanded rat bone marrow stromal cells, Exp. Neurol. 199 (2006) 416–426.

[34] T. Lonergan, C. Brenner, B. Bavister, Differentiation-related changes in mitochondrial properties as indicators of stem cell competence, J. Cell Physiol. 208 (2006) 149–153.

[35] K. Stewart, P. Monk, S. Walsh, C.M. Jefferiss, J. Letchford, J.N. Beresford, Stro1, HOP-26 (CD63), CD49a and SB-10 (CD166) as markers of primitive human marrow stromal cells and their more differentiated progeny: a comparative investigation
IN VITRO, Cell Tissue Res. 313 (2003) 281–290.

[36] K. Stenderup, J. Justesen, E.F. Eriksen, S.I. Rattan, M.-J. Kassem,
Number and proliferative capacity of osteogenic stem cells are maintained during aging and in patients with osteoporosis, Bone Miner. Res. 16 (2001) 1120–1129.

[37] A. Matityahou, N. Rosenzweig, E. Golomb, Rapid proliferation of prostatic epithelial cells in spontaneously hypertensive rats: a model of spontaneous hypertension and prostate hyperplasia,
J. Androl. 24 (2003) 263–269.

[38] S. Anoopkumar-Dukie, J.B. Carey, T. Conere, E. O'Sullivan, F.N. van Pelt, A. Allshire, Resazurin assay of radiation response in cultured cells, Br. J. Radiol. 78 (2005) 945–947.

[39] J.D. Kretlow, Y.Q. Jin, W. Liu, W.J. Zhang, T.H. Hong, G. Zhou, L.S. Baggett, A.G. Mikos, Y. Cao, Donor age and cell passage affects differentiation potential of murine bone marrow-derived stem cells, B.M.C. Cell Biol. 9 (2008) 60–73.

[40] W. Baron, B. Metz, R. Bansal, D. Hoekstra, H. de Vries, PDGF and FGF-2 signaling in oligodendrocyte progenitor cells: regulation of proliferation and differentiation by multiple intracellular signaling pathways, Mol. Cell. Neurosci. 15 (2000) 314–329.

[41] L.R. Coulthard, D.E. White, D.L. Jones, M.F. McDermott, S.A. Burchill, p38(MAPK): stress responses from molecular mechanisms to ther-apeutics, Trends Mol. Med. 15 (2009) 369–379.

[42] B.R. Chitteti, Y.H. Cheng, B. Poteat, S. Rodriguez-Rodriguez, W.S. Goebel, N. Carlesso, M.A. Kacena, E.F. Srour, Impact of interac-tions in cellular components of the bone marrow microenvir-onment on heamatopoietic stem and progenitor cell function, Blood 115 (2010) 3239–3248.

[43] B. Varnum-Finney, L.M. Halasz, M. Sun, T. Gridley, F. Radtke, I.D. Bernstein, Notch-2 governs the rate of generation of mouse long- and short-term repopulating stem cells, J. Clin. Invest. 121 (2011) 1207–1216.

[44] I. Maillard, U. Koch, A. Dumortier, O. Shestova, L. Xu, H. Sai, S.E. Pross, S.E.J.C. Aster, A. Bhandoola, F. Radtke, W.S. Pear, Canonical Notch signalling is dispensable for the maintenance of adult haematopoietic stem cells, Stem Cell 2 (2008) 356–366.

[45] M.D. Cohen, V. Ciocca, R.A. Panettieri Jr, TGF-beta 1 modulates human airway smooth-muscle cell proliferation induced by mitogens, Am. J. Respir. Cell. Mol. Biol. 16 (1997) 85–90.

[46] M.J. Robinson, M.H. Cobb, Mitogen-activated protein kinase pathways, Curr. Opin. Cell. Biol. 9 (1997)

180–186.
[47] T. Morooka, E. Nishida, Requirement of p38 mitogen-activated protein kinase for neuronal differentiation in PC12 cells, J. Biol. Chem 273 (1998) 24285–24288.
[48] M. Mohammadi, I. Dikic, A. Sorokin, W.H. Burgess, M. Jaye, J. Schlessinger, Identification of six novel autophosphorylation sites on fibroblast growth factor receptor 1 and elucidation of their importance in receptor activation and signal transduction, Mol. Cell Biol. 16 (1996) 977–989.
[49] A. Tedeschi, S. Di Giovanni, The non-apoptotic role of p53 in neuronal biology: enlightening the dark side of the moon, E.M.B.O. Rep. 10 (2009) 576–583.
[50] A. Molchadsky, N. Rivlin, R. Brosh, V. Rotter, R. Sarig, p53 is balancing development, differentiation and de-differentiation to assure cancer prevention, Carcinogenesis 31 (2010) 1501–1508.
[51] N. Almog, V. Rotter, Involvement of p53 in cell differentiation and development, Biochim Biophys. Acta 1333 (1997) F1–27.
[52] J. Choi, L.A. Donehower, p53 in embryonic development: maintaining a fine balance, Cell Mol. Life Sci. 55 (1999) 38–47.
[53] H. Li, X. Fan, R.C. Kovi, Y. Jo, B. Moquin, R. Konz, C. Stoicov, E. Kurt-Jones, S.R. Grossman, S. Lyle, A.B. Rogers, M. Montrose, J. Houghton, Spontaneous expression of embryonic factors and p53 point muta-tions in aged mesenchymal stem cells: a model of age-related tumorigenesis in mice, Cancer Res. 67 (2007) 10889–10898.
[54] A. Armesilla-Diaz, P. Bragado, I. Del Valle, E. Cuevas, I. Lazaro, C. Martin, J.C. Cigudosa, A. Silva, p53 regulates the self-renewal and differentiation of neural precursors, Neuroscience 158 (2009) 1378–1389.
[55] S. Erster, M. Mihara, R.H. Kim, O. Petrenko, U.M. Moll, IN VIVO mitochondrial p53 translocation triggers a rapid first wave of cell death in response to DNA damage that can precede p53 target gene activation, Mol. Cell. Biol. 24 (2004) 6728–6741.
[56] S. Compton, C. Kim, N.B. Griner, P. Potluri, I.E. Scheffler, S. Sen, S.D.J. Jerry, S. Schneider, N. Yadava, Mitochondrial dysfunction impairs tumor suppressor p53 expression/function, J. Biol. Chem. 286 (2011) 20297–20312.
[57] J. Campisi, Cancer and aging: yin, yang, and p53, Sci. Aging Knowledge Environ. (2002) pe1 Review.
[58] P.L. de Keizer, R.M. Laberge, J. Campisi, p53: Pro-aging or pro-longevity?, Aging (Albany NY) 2 (2010) 377–379.
[59] Z.N. Demidenko, S.G. Zubova, E.I. Bukreeva, V.A. Pospelov, T.V. Pospelova, M.V. Blagosklonny, Rapamycin decelerates cellular senescence, Cell Cycle 8 (2009) 1888–1895.
[60] Y.L. Lee, S.Y. Jeong, M. Karbowski, C.L. Smith, R.J. Youle, Roles of the mammalian mitochondrial fission and fusion mediators Fis1, Drp1, and Opa1 in apoptosis, Mol. Biol. Cell. 15 (2004) 5001–5011.
[61] M. Karbowski, R.J. Youle, Dynamics of mitochondrial morphol-ogy in healthy cells and during apoptosis, Cell Death Differ. 10 (2003) 870–880.
[62] C. Ulivieri, Cell death: insights into the ultrastructure of mitochondria, Tissue Cell 42 (2010) 339–347.
[63] K. De Vos, F. Severin, F. Van Herreweghe, K. Vancompernolle, V. Goossens, A. Hyman, J. Grooten, Tumor necrosis factor induces hyperphosphorylation of kinesin light chain and inhibits kinesin-mediated transport of mitochondria, J. Cell Biol. 149 (2000) 1207–1214.
[64] A. Varadi, L.I. Johnson-Cadwell, V. Cirulli, Y. Yoon, V.J. Allan, G.A. Rutter, Cytoplasmic dynein regulates the subcellular distribu-tion of mitochondria by controlling the recruitment of the fission factor dynamin-related protein-1, J. Cell Sci. 117 (2004) 4389–4400.
[65] W.D. Thomas, X.D. Zhang, A.V. Franco, T. Nguyen, P. Hersey, TNF-related apoptosis-inducing ligand-induced apoptosis of melanoma is associated with changes in mitochondrial mem-brane potential and perinuclear clustering of mitochondria, J. Immunol. 165 (2000) 5612–5620.
[66] M. Jendrach, S. Pohl, M. Voth, M.A. Kowald, P. Hammerstein, J. Bereiter-Hahn, Morpho-dynamic changes of mitochondria during ageing of human endothelial cells, Mech. Ageing Dev. 126 (2005) 813–821.
[67] E.E. Morrison, R.M. Costanzo, Regeneration of olfactory sensory neurons and reconnection in the aging hamster central nervous system, Neurosci. Lett 198 (1995) 213–217.

[68] J.M. Luo, Y.Q. Geng, Y. Zhi, M.Z. Zhang, N. van Rooijen, Q. Cui, Increased intrinsic neuronal vulnerability and decreased bene-ficial reaction of macrophages on axonal regeneration in aged rats, Neurobiol. Aging 31 (2010) 1003–1009.